Quantitative phase retrieval with picosecond X-ray pulses from the ATF Inverse Compton Scattering source

M. Endrizzi,[1,2,*] T. E. Gureyev,[2] P. Delogu,[3] P. Oliva,[4] B. Golosio,[4] M. Carpinelli,[4] I. Pogorelsky,[5] V. Yakimenko,[5] and U. Bottigli[1]

[1]*Dipartimento di Fisica, Università di Siena, Via Roma 56, 53100 and INFN, Sezione di Pisa 56127, Italy*
[2]*CSIRO Materials Science and Engineering, Clayton South, 3169, VIC, Australia*
[3]*Dipartimento di Fisica "E. Fermi", Università di Pisa, Largo B. Pontecorvo 3, 56127 Pisa and INFN, Sezione di Pisa 56127, Italy*
[4]*Struttura Dipartimentale di Matematica e Fisica, Università di Sassari and INFN, Sezione di Cagliari 07100, Italy*
[5]*Accelerator Test Facility, Brookhaven National Laboratory, 820, Upton, New York 11973, USA*
[*]*marco.endrizzi@pi.infn.it*

Abstract: Quantitative phase retrieval is experimentally demonstrated using the Inverse Compton Scattering X-ray source available at the Accelerator Test Facility (ATF) in the Brookhaven National Laboratory. Phase-contrast images are collected using in-line geometry, with a single X-ray pulse of approximate duration of one picosecond. The projected thickness of homogeneous samples of various polymers is recovered quantitatively from the time-averaged intensity of transmitted X-rays. The data are in good agreement with the expectations showing that ATF Inverse Compton Scattering source is suitable for performing phase-sensitive quantitative X-ray imaging on the picosecond scale. The method shows promise for quantitative imaging of fast dynamic phenomena.

OCIS codes: (110.7440, 170.7440) X-ray imaging; (100.5070) Phase retrieval.

References and links

1. H. Ikeura-Sekiguchi, R. Kuroda, M. Yasumoto, H. Toyokawa, M. Koike, K. Yamada, F. Sakai, K. Mori, K. Maruyama, H. Oka, and T. Kimata, "In-line phase-contrast imaging of a biological specimen using a compact laser-compton scattering-based x-ray source," Appl. Phys. Lett. **92**, 131107 (2008).
2. P. Oliva, B. Golosio, S. Stumbo, A. Bravin, and P. Tomassini, "Compact x-ray sources for mammographic applications: Monte Carlo simulations of image quality," Med. Phys. **36**, 5149–5161 (2009).
3. A. Snigirev, I. Snigireva, V. Kohn, S. Kuznetsov, and I. Schelokov, "On the possibilities of x-ray phase contrast microimaging by coherent high-energy synchrotron radiation," Rev. Sci. Instrum. **66**, 5486–5492 (1995).
4. S. W. Wilkins, T. E. Gureyev, D. Gao, A. Pogany, and A. W. Stevenson, "Phase-contrast imaging using polychromatic hard x-rays," Nature **384**, 335–338 (1996).
5. P. Cloetens, R. Barrett, J. Baruchel, J.-P. Guigay, and M. Schlenker, "Phase objects in synchrotron radiation hard x-ray imaging," J. Phys. D Appl. Phys. **29**, 133 (1996).
6. K. A. Nugent, T. E. Gureyev, D. F. Cookson, D. Paganin, and Z. Barnea, "Quantitative phase imaging using hard x rays," Phys. Rev. Lett. **77**, 2961–2964 (1996).
7. R. Fitzgerald, "Phase-sensitive x-ray imaging," Phys. Today **53**, 23–26 (2000).
8. S. Mayo, T. Davis, T. Gureyev, P. Miller, D. Paganin, A. Pogany, A. Stevenson, and S. Wilkins, "X-ray phase-contrast microscopy and microtomography," Opt. Express **11**, 2289–2302 (2003).

#137598 - $15.00 USD Received 2 Nov 2010; revised 25 Nov 2010; accepted 27 Nov 2010; published 28 Jan 2011

9. I. V. Pogorelsky, I. Ben-Zvi, T. Hirose, S. Kashiwagi, V. Yakimenko, K. Kusche, P. Siddons, J. Skaritka, T. Kumita, A. Tsunemi, T. Omori, J. Urakawa, M. Washio, K. Yokoya, T. Okugi, Y. Liu, P. He, and D. Cline, "Demonstration of $8\times10^{18} photons/second$ peaked at 1.8 å in a relativistic thomson scattering experiment," Phys. Rev. ST Accel. Beams **3**, 090702 (2000).
10. P. Oliva, M. Carpinelli, B. Golosio, P. Delogu, M. Endrizzi, J. Park, I. Pogorelsky, V. Yakimenko, O. Williams, and J. Rosenzweig, "Quantitative evaluation of single-shot inline phase contrast imaging using an inverse compton x-ray source," Appl. Phys. Lett. **97**, 134104 (2010).
11. O. Williams, G. Andonian, M. Babzien, E. Hemsing, K. Kusche, J. Park, I. Pogorelsky, G. Priebe, J. Rosenzweig, and V. Yakimenko, "Characterization results of the bnl atf compton x-ray source using k-edge absorbing foils," Nucl. Instrum. Methods Phys. Res. A **608**, S18 – S22 (2009). Compton sources for X/[gamma] rays: Physics and applications.
12. E. Esarey, S. K. Ride, and P. Sprangle, "Nonlinear thomson scattering of intense laser pulses from beams and plasmas," Phys. Rev. E **48**, 3003–3021 (1993).
13. W. J. Brown, S. G. Anderson, C. P. J. Barty, S. M. Betts, R. Booth, J. K. Crane, R. R. Cross, D. N. Fittinghoff, D. J. Gibson, F. V. Hartemann, E. P. Hartouni, J. Kuba, G. P. Le Sage, D. R. Slaughter, A. M. Tremaine, A. J. Wootton, P. T. Springer, and J. B. Rosenzweig, "Experimental characterization of an ultrafast thomson scattering x-ray source with three-dimensional time and frequency-domain analysis," Phys. Rev. ST Accel. Beams **7**, 060702 (2004).
14. W. J. Brown and F. V. Hartemann, "Three-dimensional time and frequency-domain theory of femtosecond x-ray pulse generation through thomson scattering," Phys. Rev. ST Accel. Beams **7**, 060703 (2004).
15. T. E. Gureyev, "Transport of intensity equation for beams in arbitrary state of temporal and spatial coherence," Optik **110**, 263–266 (1999).
16. D. Paganin, S. C. Mayo, T. E. Gureyev, P. R. Miller, and S. W. Wilkins, "Simultaneous phase and amplitude extraction from a single defocused image of a homogeneous object," J. Microsc. **206**, 33–40 (2002).
17. U. W. Arndt and B. T. M. Willis, *Single Crystal Diffractometry* (Cambridge University Press, Cambridge, 1966).

1. Introduction

Inverse Compton Scattering (ICS) represents a promising method for producing near-monochromatic and intense X-ray pulses. This method has received considerable interest in the last few years for high-quality X-ray imaging applications [1, 2]. From the imaging point of view, the main features of this kind of X-ray source are the near-monochromaticity, the tunable peak energy, the small source size, the high intensity and the short duration of the X-ray pulses. Among the various techniques that can be used to obtain phase-contrast X-ray images, the so called in-line imaging is the simplest in principle and easiest to implement [3–6]. Phase-contrast imaging is a valuable tool for enhancing the contrast especially when the samples to be visualized are weakly absorbing (low Z), hence clinical and biological studies benefit from the development of phase-sensitive imaging techniques [7]. Phase retrieval enables the recovery of quantitative information from phase-contrast images and improves the quality of tomographic reconstruction [5–8].

2. Materials and methods

The X-ray source used in this study is the ICS source available at the Accelerator Test Facility in the Brookhaven National Laboratory [9]. The imaging setup and the source characteristics have been described elsewhere [9, 10], a brief summary of the various parameters of our experiment is here reported. The electron beam energy is 79 MeV with 0.15% energy spread and focus spot size of $32\,\mu$m. The CO_2 laser pulses ($10.6\,\mu$m wavelength) are focused into a $40\,\mu$m rms spot in head-on collision geometry. The peak energy of the X-ray beam can be computed as [11]:

$$E_{X-ray} = E_{laser}\frac{4\gamma^2}{1+(a_L^2/2)+(\theta\gamma)^2} \tag{1}$$

which gives 10.4 keV. In Eq. (1) E_{X-ray} is the scattered X-ray energy, E_{laser} is the laser photon energy, γ is the electron beam Lorentz factor, a_L is the normalized laser vector potential [12]

#137598 - $15.00 USD Received 2 Nov 2010; revised 25 Nov 2010; accepted 27 Nov 2010; published 28 Jan 2011

and θ is the observation half-angle. The total number of photons is expected to be 10^8 per pulse. The pulse duration is about 1 picosecond [10].

The source is located at the position $-r_1 = -1050$ mm along the z axis which coincides with the beam axis. The object is positioned at the origin and the detector is placed in a plane (x,y) orthogonal to the beam axis at $r_2 = 2235$ mm. The objects to be analyzed are polymer wires (cylinders) of various thicknesses: two samples made of Nylon with diameters 170 and 535 μm, two samples made of PET (polyethylene terephthalate) with diameters 107 and 520 μm and one sample of PMMA (polymethyl methacrylate) with diameter 1124 μm. These polymers are composed of low-Z elements including hydrogen, oxygen and carbon which are also the main components of many biological soft tissues.

The imaging detector is a flat panel (Hamamatsu $C9728DK-10$) based on a CMOS sensor coupled with a scintillator (CsI). The detector Line Spread Function (LSF) is well approximated by two Gaussian functions ($\sigma_1 = 40, \sigma_2 = 101\,\mu$m, relative amplitude $A_2/A_1 = 0.4$). Each image is acquired with a single shot and the detector acquisition is manually synchronized with the X-ray pulse. The image is equalized using an estimated "flat-field" (the image acquired without the object). The pixels that contain any detail of the sample are excluded from the data set and a two-dimensional Gaussian function is fitted to the remaining part of the experimental image. This estimates the intensity distribution that would have been detected without the object. The model for the intensity distribution is chosen as a two-dimensional Gaussian function. This choice can be justified looking at the flat-field: the intensity profiles along two orthogonal directions in the (x,y) plane are well fitted with a Gaussian distribution if we allow two different widths to be used. The same choice has been reported in a previous work [13]. This fitting procedure is necessary to equalize the detail of the image for which an experimental flat-field is not available. The actual shot-to-shot reproducibility (in terms of shape, position and intensity) is not good enough for a conventional flat-field equalization.

The ideal kinematic spectrum of an ICS source is significantly broadened at any observation position by the three-dimensional effects of the collision [14]. The observation angle can be chosen such that the energy spread due to the three-dimensional effects ($\Delta' E/E$) becomes comparable to the energy spread due to the geometry-dependent relativistic Doppler up-shift of the scattered photons ($\Delta'' E/E$). The spectral broadening of our X-ray beam is [9,14] $\Delta' E/E \approx 0.6\%$ and the same bandwidth is observed over an angle $\theta = 0.5$ mrad such that $\Delta'' E/E \approx \gamma^2\theta^2$. Within an angle of ~ 1 mrad the position-dependent energy spread is directly comparable to the spectral broadening expected from the three-dimensional effects.

With an ICS source it is possible to realize phase-contrast imaging using a single X-ray pulse [10]. Applying phase retrieval to such fast images gives quantitative information about the sample with a time resolution which is on the picosecond scale. As the X-ray spectrum produced by an ICS source is both polychromatic and spatially variant, it is necessary to analyse the conditions for applicability of previously reported phase-retrieval methods to images obtained with the use of such sources. Here we present such analysis in the case of phase retrieval based on the Transport of Intensity Equation (TIE). The TIE that can be derived under the assumptions of a homogeneous object and paraxial incident illumination is [15, 16]:

$$S_1(x,y;\nu) = \left(1 - \frac{R'c}{4\pi\nu}\frac{\delta(c/\nu)}{\beta(c/\nu)}\nabla^2\right) S_0(x,y;\nu) \tag{2}$$

where $S_0(x,y;\nu)$ is the spectral density in the plane in contact with the object, $S_1(x,y;\nu)$ is the spectral density of the transmitted X-ray wave at a given position (x,y) in a plane perpendicular to the X-ray beam propagation axis, at a distance r_2 from the object and $R' = r_1 r_2/(r_1 + r_2)$ is the defocus distance. $S_0(x,y;\nu)$ can be expressed in terms of the incident spectral density S_{in} and the projected thickness $T(x,y)$ of the object as $S_0(x,y;\nu) =$

#137598 - $15.00 USD Received 2 Nov 2010; revised 25 Nov 2010; accepted 27 Nov 2010; published 28 Jan 2011

$S_{in}(x,y;\nu)\exp\{-(4\pi\nu/c)\beta(c/\nu)T(x,y)\}$. The refractive index of the sample material is defined as $n(c/\nu)=1-\delta(c/\nu)+i\beta(c/\nu)$ and $\nu=c/\lambda$ is the frequency of a given monochromatic component (c is the speed of light).

Outside the absorption edges, $\beta(c/\nu)$ and $\delta(c/\nu)$ can be approximated as $\beta(c/\nu)=(\nu_0/\nu)^4\beta(c/\nu_0)$ and $\delta(c/\nu)=(\nu_0/\nu)^2\delta(c/\nu_0)$ [17]. We choose ν_0 as the peak frequency of the X-ray beam. With integration of Eq. (2) over the frequency and using $\mu=4\pi\beta/\lambda$, the expression for the intensity becomes ($I(x,y)=\int S(x,y;\nu)d\nu$):

$$I_1(x,y)=I_0(x,y)-\frac{R'\delta(c/\nu_0)}{\mu(c/\nu_0)}\nabla^2\int\frac{\nu}{\nu_0}S_0(x,y;\nu)d\nu. \tag{3}$$

In order to substitute ν/ν_0 with 1 in Eq. (3) the inequality (relative error) to be satisfied is:

$$\left|\nabla^2\int S_0(x,y;\nu)\left[\frac{\nu}{\nu_0}-1\right]d\nu\right|<<\frac{\mu(c/\nu_0)}{R'\delta(c/\nu_0)}. \tag{4}$$

With the condition in Eq. (4), Eq. (3) can be expressed as:

$$I_1(x,y)\approx I_0(x,y)-\frac{R'\delta(c/\nu_0)}{\mu(c/\nu_0)}\nabla^2 I_0(x,y) \tag{5}$$

that is valid provided that a sufficiently small region is selected in the image, in which the frequency does not change too much:

$$a\frac{\Delta E_{max}}{E_0}\frac{\delta(c/\nu_0)}{\beta(c/\nu_0)}\frac{1}{N_F}<<1 \tag{6}$$

where $N_F=4\pi h^2/(\lambda_0 R')$, $a=h^2\left|\nabla^2 I(x,y)\right|$ and h is the size of the smallest resolvable detail in the object plane. In our experiment the maximum value of the left-hand side of condition (6) is less than 5×10^{-4}. Equation (5) can be solved for I_0 using the Fourier transform [16] and, once $I_0(x,y)$ is known, the projected thickness $T(x,y)$ is recovered with the relation ($I_{in}(x,y)=\int S_{in}(x,y;\nu)d\nu$):

$$T(x,y)=-\frac{1}{\mu(c/\nu_0)}\ln\left(\frac{I_0(x,y)}{I_{in}(x,y)}\right). \tag{7}$$

3. Results

A single-shot image of the PMMA sample is presented in Fig. 1. The raw acquisition is reported

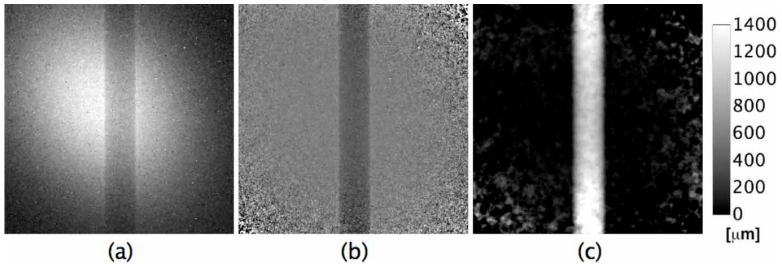

Fig. 1. Single-shot image of the PMMA sample. (a) Raw acquisition corrected for the dark current. (b) Equalized intensity distribution. (c) Reconstructed projected thickness.

together with the equalized intensity distribution and the reconstructed projected thickness. The

#137598 - $15.00 USD Received 2 Nov 2010; revised 25 Nov 2010; accepted 27 Nov 2010; published 28 Jan 2011

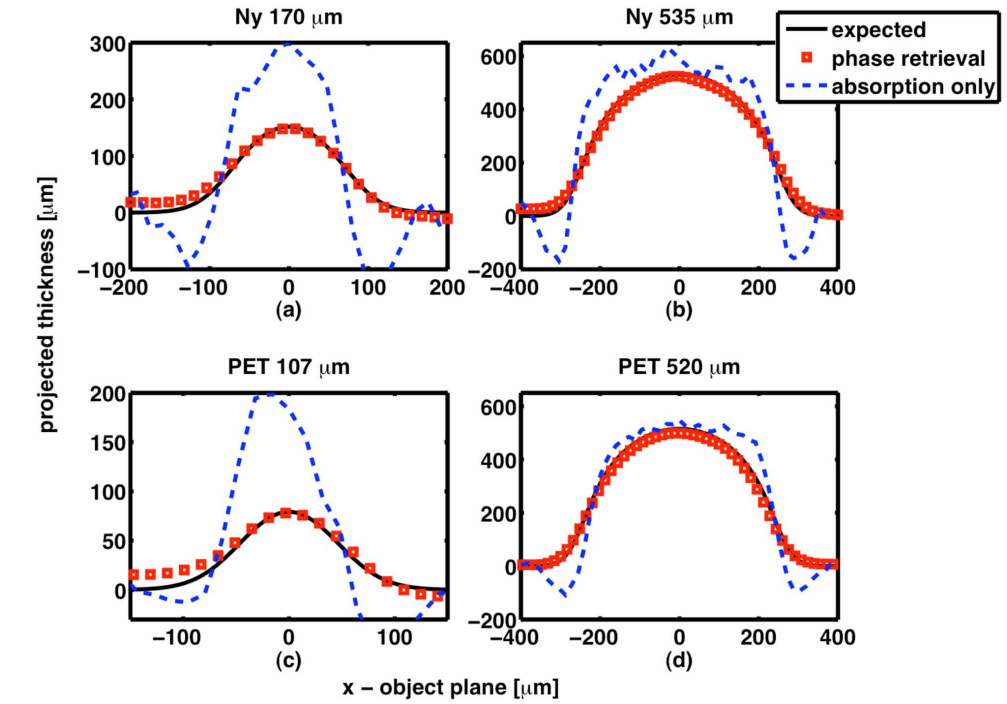

Fig. 2. Reconstructed projected thickness at the object plane. (a) Nylon 170 μm. (b) Nylon 535 μm. (c) PET 107 μm. (d) PET 520 μm. The reconstruction after phase retrieval is compared to the reconstruction using only absorption.

profiles of the various samples have been extracted for a quantitative comparison between the known projected thicknesses and the ones reconstructed using Eq. (5) and Eq. (7) (Fig. 2 and Fig. 3). The expected profile is computed as the wire projected thickness convoluted with the system LSF. The indexes of refraction used for the reconstruction are $\delta = \{2.76, 2.38, 2.47\} \times 10^{-6}$ and $\beta = \{3.94, 2.64, 3.28\} \times 10^{-9}$ for PET, Nylon and PMMA respectively.

The maximum thickness is estimated with less than 3% relative error for all the samples, while the whole profile is accurate only for the thicker samples. The profiles are averaged over 50 rows across the wires, as close as possible to beam axis; for the PET 107 μm sample the average is taken over a larger number of rows (100) because of the smaller signal-to-noise ratio achieved. The thinner wires have a diameter which is comparable to the resolution of our imaging system; a small error in the characterization of the system point-spread function would result in considerable discrepancies between the expected and the measured projected intensities. The spot size depends on the overlap of the electron bunch and the laser pulse and can fluctuate from shot to shot. This could explain the relatively less accurate reconstruction obtained with those samples. An asymmetry can be noted in (a), (b) and (c) frames of Fig. 2. Since the phase retrieval procedure cannot introduce any asymmetry by itself, we consider this effect to be a consequence of the non-perfect image equalization.

The projected thicknesses can also be computed using only the information coming from absorption (Fig. 2 and Fig. 3). These profiles are averaged over the same regions previously selected on the images processed with phase retrieval. Because of the fringes that are present in the image ($I_1(x,y)$), the projected thickness appears to be negative in the region near the phase edge (air-polymer interface). This clearly leads to a non-physical measure of the thick-

#137598 - $15.00 USD Received 2 Nov 2010; revised 25 Nov 2010; accepted 27 Nov 2010; published 28 Jan 2011

ness. Nevertheless we can still compare the results far away from the edges by estimating the maximum projected thickness obtained with phase retrieval and with absorption only. The profiles obtained using only absorption are much less accurate than the ones obtained with phase retrieval, especially in the cases of the thinner wires. Note also that the profiles for the absorption analysis are noisier than those measured after phase retrieval. This is a consequence of the smoothing properties of the phase retrieval process. The asymmetries of the projected thickness profiles reconstructed after phase retrieval ((a),(b) and (c) Fig. 2) are present also in the pure absorption profiles. This is a confirmation that a non-perfect equalization led to an asymmetric intensity profile $I_1(x,y)$.

The same results are reported in Fig. 3 for the PMMA wire. In this case also a single-row

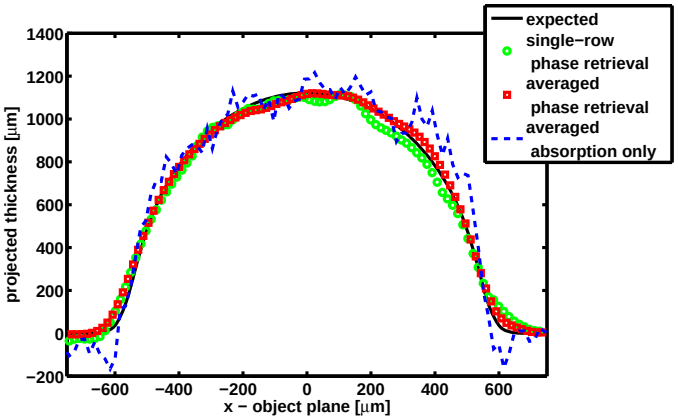

Fig. 3. PMMA wire (1124 μm) reconstruction. The single-row profile and the averaged profile measured using phase retrieval are compared to the estimation obtained using only absorption.

profile is presented. Averaging the profiles near the center of the beam produces a better result. It is also possible to note that for this sample the effects due to the phase are restricted to the air-polymer interface and the central part of the wire can be considered affected only by absorption.

4. Conclusions

Quantitative phase retrieval has been experimentally demonstrated on homogeneous samples of different polymers using an Inverse Compton Scattering X-ray source. The recovered projected thicknesses are shown to be in good agreement with the expectation, demonstrating that quantitative information about homogeneous samples can be obtained on the picosecond time scale with this kind of source. The results have been also compared with an analysis based only on absorption: phase retrieval leads to a much more accurate estimation, especially when the details to be detected are small (few hundreds of microns). The possibility to perform phase retrieval on phase-contrast images will be useful for quantitative computed tomography applications with ICS sources.

Acknowledgments

ME and TEG acknowledge the support from CSIRO Computational and Simulation Sciences Transformational Capability Platform.

#137598 - $15.00 USD Received 2 Nov 2010; revised 25 Nov 2010; accepted 27 Nov 2010; published 28 Jan 2011